Ginzburg-Landau Parameters of Type-II Superconductors*

T. McConville†‡ and B. Serin

Rutgers, The State University, New Brunswick, New Jersey

(Received 21 April 1965)

Specific heats in a magnetic field were measured for three specimens of niobium, a 50% Nb–50% Ta specimen, and an In+1.9% Bi specimen. These data were supplemented by magnetization measurements on one niobium specimen. From the data, two Ginzburg-Landau parameters are calculated: K_1, determined by the magnitude of the upper critical field, and K_2, determined by the slope of the magnetization curve at this field. For the niobium specimens, K_2 exceeds K_1 at all temperatures below the transition temperature, in qualitative agreement with the theory of pure type-II superconductors of Maki and Tsuzuki. The ratio K_2/K_1 at a given temperature is largest in the purest Nb and less in impure Nb. In the pure specimens, the temperature dependence of K_1 is more rapid than predicted by theory, the experimental value of $K_1(0)$ being about 25% larger than the theoretical value of 0°K. For the alloy specimens, $K_2 \sim K_1$, over the temperature range measured, and both parameters increase with decreasing temperature. This result contradicts the inequality $K_2 < K$ (where K is the Ginzburg-Landau parameter at T_c) derived by Maki for type-II superconductors of short electron mean free path.

I. INTRODUCTION

DURING the past few years there has been great interest in the properties of type-II superconductors.[1] Their magnetization curves have been determined in most investigations. Generally speaking, these data support the description of type-II behavior derived by Abrikosov,[2] and many of the results obtained by Gor'kov[3,4] from the microscopic theory of superconductivity.

There have been relatively fewer investigations of the specific heats of type-II materials in a magnetic field. The measurements of Morin *et al.*[5] on the heat capacity of V_3Ga were the first made explicitly to clarify the properties of hard superconductors. Similar results had been obtained earlier in impure tantalum[6] and in vanadium,[7] but their meaning was not appreciated at the time. Goodman[8] pointed out that the data for V_3Ga could be understood on the basis of Abrikosov's theory. Recently, Hake and Brammer[9] determined the specific heats of a well-annealed V+5% Ta specimen, and found good agreement with the Abrikosov description.

---

[1] See, e.g., Proceedings of the Conference on the Science of Superconductivity, Hamilton, New York, 1963 [Rev. Mod. Phys. 36, (1964)].

[2] A. A. Abrikosov, Zh. Eksperim. i Teor. Fiz. 32, 1442 (1957) [English transl.: Soviet Phys.—JETP 5, 1174 (1957)]; J. Phys. Chem. Solids 2, 199 (1957).

[3] L. B. Gor'kov, Zh. Eksperim. i Teor. Fiz. 37, 1407 (1959) [English transl.: Soviet Phys.—JETP 10, 998 (1960)].

[4] L. B. Gor'kov, Zh. Eksperim. i Teor. Fiz 37, 833 (1959) [English transl.: Soviet Phys.—JETP 10, 593 (1960)].

[5] F. J. Morin, J. P. Maita, H. J. Williams, R. C. Sherwood, J. H. Wernick, and J. E. Kunzler, Phys. Rev. Letters 8, 275 (1962).

[6] W. H. Keesom and M. Désirant, Physica 8, 273 (1941).

[7] W. S. Corak, B. B. Goodman, C. B. Satterthwaite, and A. Wexler, Phys. Rev. 102, 656 (1956).

[8] B. B. Goodman, Phys. Letters 1, 215 (1962).

[9] R. R. Hake and W. G. Brammer, Phys. Rev. 133, A719 (1964); R. R. Hake, Rev. Mod. Phys. 36, 124 (1964).

In this paper we describe in detail specific-heat measurements on various specimens of niobium, a 50% Nb–50% Ta specimen, and an alloy of indium. Magnetization data have also been obtained on a specimen of pure niobium. Preliminary brief reports on the thermal measurements have already appeared.[10,11] Since these reports, the theory has been extended, and we have recalculated the data and put them in a form which permits comparison with these most recent theoretical results. The new magnetization measurements have been obtained at lower temperatures than could be reached with the specific-heat apparatus.

Stromberg and Swenson[12] first reported that very pure niobium exhibits type-II magnetic behavior. Niobium is an interesting material because it is a rare example of an intrinsic type-II superconductor. That is to say, even the purest specimens, in which the electron mean free path is very long, exhibit type-II properties. Most other type-II superconductors are alloys in which the electron mean free path is quite short. We shall show that in certain respects niobium behaves qualitatively differently from the alloy specimens. The data we have obtained permit a critical comparison with some aspects of the detailed microscopic theoretical treatments of type-II behavior which have recently appeared.

II. RELATIONS USED FOR ANALYZING THE DATA

According to Abrikosov,[2] type-II superconductors can be described by a single parameter—the Ginzburg-Landau parameter[13] K. For such superconductors $K > 1/\sqrt{2}$. A magnetization curve for niobium is shown in Fig. 5. All type-II superconductors exhibit qualita-

---

[10] T. McConville and B. Serin, Rev. Mod. Phys. 34, 112 (1964).

[11] T. McConville and B. Serin, Phys. Rev. Letters 13, 365 (1964).

[12] T. F. Stromberg and C. A. Swenson, Phys. Rev. Letters 9, 370 (1962).

[13] V. L. Ginzburg and L. D. Landau, Zh. Eksperim. i Teor. Fiz. 20, 1064 (1950).

tively similar behavior. At a fixed temperature below transition temperature T_c and in increasing magnetic field, a long cylindrical specimen is a perfect diamagnetic until the lower critical field $H_{c1}(T)$ is reached. At this point a phase transition occurs from the superconducting to the mixed state, and magnetic flux begins to enter the specimen in the form of fluxoids. The mixed state persists until the field reaches the value $H_{c2}(T)$ when a second phase transistion into the normal state occurs. Between H_{c1} and H_{c2} the magnetization changes from $-H_{c1}/4\pi$ to zero. In keeping with recent discussions of Maki,[14,15] in what follows we generalize the theory of Abrikosov, and permit the possibility that different features of the magnetization curve are described by different values of the parameter K, which may depend on temperature in different ways. The two Ginzburg-Landau parameters used, K_1 and K_2, are defined by Eqs. (1) and (6) below.

Specific-heat measurements are usually made in a constant applied magnetic field H_a while the temperature is varied. As can be seen in Fig. 3, beginning at low temperature, the specific heat increases with temperature in a smooth manner until the temperature is reached for which $H_{c1}(T) = H_a$. At this point the specific heat shows a very large narrow peak. This is followed by another slow change until the temperature for which $H_{c2}(T) = H_a$. At this temperature, the specific heat drops discontinuously to its value in the normal state. Such a discontinuous specific-heat jump is characteristic of second-order transitions. The behavior of the magnetization and of the specific heat are related through thermodynamics, as will be described below.

Theory[2] relates the upper critical field $H_{c2}(T)$ to the thermodynamic critical field $H_c(T)$ through the relation

$$H_{c2}(T) = \sqrt{2}K_1(T)H_c(T). \tag{1}$$

H_{c2} can be determined directly from the magnetization curve from the applied field at which the moment vanishes. For the specific-heat measurements, since $H_{c2}(T) = H_a$, at the temperature T_H of the second-order specific-heat discontinuity, the upper critical field is also directly measured. Thus, Eq. (1) can be used to find $K_1(T)$ once $H_c(T)$ is known. To find H_c, we use the fact that the slope of the thermodynamic critical field $(dH_c/dT)_{T_c}$ can be determined by means of the Rutgers formula[16] from the magnitude of the discontinuity in specific heat $(\Delta C/VT)_{T_c}$ which occurs at the transition temperature in the absence of a field, and which we also measure (see Fig. 2). This formula is

$$(\Delta C/VT)_{T_c} = (1/4\pi)(dH_c/dT)^2_{T_c}. \tag{2}$$

To determine $H_c(T)$, we assume that the critical field curve is a parabolic function of temperature,

$$H_c(T) = H_0[1 - (T/T_c)^2], \tag{3}$$

and determine H_0, the critical field at 0°K, so that the foregoing value of $(dH_c/dT)_{T_c}$ is obtained from Eq. (3). Within experimental error, near T_c the upper critical field varies linearly with temperature. We can write

$$H_{c2} = \alpha(T_c - T). \tag{4}$$

Equations (1), (3), and (4) can be combined to give

$$\sqrt{2}K_1 = \alpha T_c/H_0(1+t), \tag{5}$$

where $t = T/T_c$. We use Eq. (5) to find K_1 from the specific-heat data. Since the magnetization measurements were made at small t, Eqs. (1) and (3) only are used. The possible errors in K_1 that can result from the use of Eq. (3). are discussed in Sec. C; we estimate that they do not exceed a few percent.

The theory[2] also predicts that the slope of the magnetization curve in the mixed state near $H_{c2}(T)$ is linear in field and is given by

$$(dM/dH)_{Hc2} = [4\pi\beta(2K_2^2(T) - 1)]^{-1}. \tag{6}$$

β is determined by the geometrical arrangement of fluxoids in the mixed state. Although different values of β have been found,[2,17] the differences are small and will not affect our conclusions. $\beta = 1.18$, as calculated by Abrikosov,[2] will be used.

By using Eq. (6), K_2 can be determined directly from the magnetization curve. For the specific-heat data, we use the fact that the phase transition at H_{c2} is second order, so that the Ehrenfest relation[8,18] connects the magnitude of the specific-heat discontinuity at T_H to the slope of the magnetization curve according to the equation

$$(\Delta C/VT)_{T_H} = (dH_{c2}/dT)^2_{T_H}(dM/dH)_{Hc2}. \tag{7}$$

Since $(dH_{c2}/dT) = -\alpha$ near T_c, Eqs. (6) and (7) can be combined to permit $K_2(T)$ to be calculated in the neighborhood of the transition temperature. Since we must use α to find K_2, it seems most consistent to use it also to find K_1.

According to the recent theoretical treatments of Maki,[14,15] at the transition temperature $K_1(T_c) = K_2(T_c) = K$. K is the parameter which appears in the Ginzburg-Landau equations which were used by Abrikosov. We remind the reader that K_1 is determined by H_{c2} and K_2 by the slope of the magnetization curve at the upper critical field.

III. EXPERIMENTAL

A. Apparatus

A diagram of the apparatus used to determine specific heats is shown in Fig. 1. The specimen (Sp) was mounted in a copper cap containing the heater (H₁) and a $\frac{1}{10}$-W Allen Bradley resistor (T) which

[14] K. Maki, Physics **1**, 21 (1964).
[15] K. Maki and T. Tsuzuki, Phys. Rev. **139**, A868 (1965).
[16] See, e.g., E. A. Lynton, *Superconductivity* (John Wiley & Sons, Inc., New York, 1962), p. 15.

[17] J. Matricon, Phys. Letters **9**, 289 (1964).
[18] P. Ehrenfest, Proc. Roy. Neth. Acad. Sci., Amsterdam **36**, 153 (1933).

served as the secondary thermometer. The specimen and addenda were rigidly connected to the plunger (P) by a thin-walled stainless steel tube (SS). The plunger was thermally anchored to the calorimeter top by copper straps at the radiation shield (R). Leads to the specimen were thermally anchored at the heat station (HS). The plunger went from the calorimeter top to the Dewar cap in a vacuum jacket (J) and came out through an "O" ring seal. The top containing the heat station and plunger was sealed in the flange (S) with indium solder. The can was then evacuated at room temperature through the tube (E). This tube also contained the capillaries (C), connecting the helium vapor pressure bulb (V) and the helium gas thermometer bulb (B) to the external manometers. With the plunger to serve as a heat switch, the specimen and carbon thermometer could be brought to the temperature of of the primary thermometers without exchange gas.

When the plunger was pushed down, the specimen was seated on a soft annealed gold disk (D) which was cemented with Apieson "N" grease to the primary thermometers. Then the specimen assembly was in good thermal contact with the gas bulbs for calibration of the carbon resistor. When the plunger was pulled up, the specimen was somewhat isolated from the calorimeter, the only heat leak being through the stainless steel tube. It was in this position that the heat capacity was measured.

The temperature of the calorimeter could be controlled with the heaters (H_2, H_3). In the region below 4.2°K, the liquid-helium level was above the can and the lower heater (H_3) stirred the liquid. In the region above 4.2°K the helium level was below the can on the brass heat leak (L), and the temperature of the can was controlled with the upper heater (H_2). As the specimen was heated in the heat-capacity measurement, the calorimeter can was also heated to keep the heat leak through the stainless steel tube to a minimum.

The magnet used in these measurements was a superconducting niobium solenoid 6 in. long and 2.5 in. in diameter. It was made to fit around the calorimeter can without touching it, so that the magnet could be kept cooler than the calorimeter. The magnet was suspended from a yoke fastened to the vacuum jacket (J) in Fig. 1. The normal Garrett[19] type of overwind was not used because of the proximity of the solder seal (S). In the designing of the solenoid, the size and placement of the overwind was varied to cancel out the effect of the superconducting ring so that the resultant field would vary over the length of a 2-in.-long specimen by only $\pm 1\%$. Because of the limited current-carrying capacity of this solenoid, H_{c2} for the niobium specimens could be achieved only down to temperatures of about 6.5°K.

The power supplied to the heater and the subsequent resistance change in the carbon thermometer were
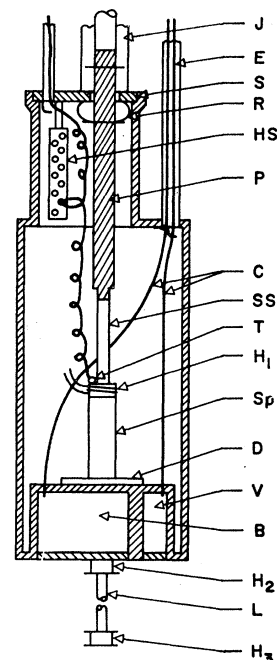

FIG. 1. Calorimeter used to determine specific heats.

measured by standard potentiometric methods. It was found that a 100-Ω Allen-Bradley resistor gave satisfactory sensitivity in the 6 to 12°K region and also was of small enough resistance at 2°K so that the time of response of the Leeds and Northrup Microvolt Amplifier in the potentiometer circuit was not appreciably affected. Thus, the one resistor was used between 2 and 20°K. Since the resistance versus temperature characteristic of resistors can change appreciably on cycling from room to low temperatures, they were calibrated against the primary thermometers in each run.

Two primary thermometers were used. At temperatures between 2.3 and 4.2°K the vapor pressure of He⁴ was used. A small amount of liquid helium was condensed in the vapor pressure bulb and the pressure was read on a mercury manometer with a cathetometer to ± 0.02 mm. Below the λ point the pressure of the helium bath itself was measured with an oil manometer. The pressure of the bath was stabilized by controlling the pumping rate.

Above 4.2°K a constant-volume helium gas thermometer served as the primary standard. The gas thermometer had a large room-temperature dead space. It was filled to a pressure of about 70 cm of mercury at room temperature, and the temperature and pressure were carefully measured. The pressure and temperature were again measured at the normal boiling point of liquid helium. From these data the ratio of the volume of the thermometer bulb to the dead volume may be calculated. This ratio being known, the absolute temperature of the bulb may be calculated from the pressure using the procedure of Franck and Martin[20]

[19] M. W. Garrett, J. Appl. Phys. **22**, 1091 (1951).

[20] J. P. Franck and D. L. Martin, Can. J. Phys. **39**, 1320 (1961).

TABLE I. Properties of specimens (ρ = resistivity, T_c = transition temperature, ΔC = specific-heat discontinuity at T_c, H_0 = calculated thermodynamic critical field at $0°K$, K = Ginzburg-Landau parameter at T_c, and α = slope of upper critical field curve at T_c).

Specimen[a]	$\dfrac{\rho\,(295°K)}{\rho\,(4.2°K)}$	T_c (°K)	$(\Delta C/VT)_{T_c}$ [mJ/cm³(°K)²]	H_0 (Oe)	K	α (Oe/°K)
Nb-4	520	9.23	1.52	2040	0.85	533
Nb-3	>500	9.23	1.52	2040	0.85	533
Nb-2	70	9.18	1.52	2040	0.96	600
50% Nb-50% Ta	6.0	6.25	1.20	1220	3.90	2150
In+1.9 at. % Bi	~2.3	3.86	0.24	336	0.97	239

[a] Descriptions are Nb-4: Composite specimen of 20 wires, each 0.07 cm diam by 2.4 cm long. Nb-3: rod, 0.6 cm diam by 5.4 cm long. With our eddy-current decay apparatus we could only set an upper limit to the resistivity of this specimen. Nb-2: rod, 0.3 cm diam by 2.1 cm long. 50% Nb-50% Ta: rod, 0.6 cm diam by 3.5 cm long. In+1.9 at. % Bi: rod, 0.6 cm diam by 5.1 cm long.

to take account of the nonideality of the helium gas. Other corrections, such as a capillary correction, a correction for the thermo-molecular pressure gradient in the capillary, and a correction for the shrinkage of the low-temperature gas bulb were found to be negligible. A standard error analysis led to a probable error in the temperatures determined with the gas thermometer of 0.5%.

The temperature T^* determined from the resistance of the carbon thermometer was obtained to a first approximation by fitting the resistance-versus-temperature data at two points to the two-constant Clement-Quinnell equation.[21] Since this equation only approximates the temperature dependence of the resistor, the resistor was compared to the temperature T of the primary thermometers at several temperatures. Then, the temperature difference $(T-T^*)$ was plotted as a function of T^* as determined by the resistor. From the resulting curve any value of T^* as determined by the resistor could be converted to absolute temperature.

The method of taking and analyzing the heating curves was very similar to that described by Gayley et al.[22] The procedure was to record the specimen temperature for a time before, during, and after the heating interval. The temperature drift before and after the heat input gave an approximate measure of the rate at which the specimen was gaining heat from or losing heat to the surroundings. The preheating temperature drift was adjusted to nearly zero. The rate of heat loss after heating was inversely proportional to the mass of the specimen. By extrapolating the pre- and post-heating curves to the mid-time of the heating interval, a measure of the temperature change caused by only the heater power was obtained. How accurately the temperature change ΔT could be determined depended on the post-cooling rate. The errors in the estimates of ΔT ranged from 1% for the larger specimens to 3% for the smallest one. The scatter in the data points was in agreement with these estimates. The uncertainties in the other factors determining C_p are small by com-

parison. The error in the measurement of the heat energy input was about 0.1%. The uncertainties in the absolute temperature made negligible contributions to the error in the temperature difference for $\Delta T < 0.2°$. Therefore, the accuracy of C_p varied from about 1 to 3% depending on the mass of the specimen.

To determine the magnetization curves of a niobium specimen, a magnetometer of simple design was used. It consisted of two coils of many turns of copper wire rigidly mounted in the solenoid which provided the magnetic field. The coils were connected to a galvanometer, and the deflection was noted when the specimen was pulled from between them. In this apparatus the solenoid was wound from Nb-Zr superconducting wire. The solenoid, detection coils, and specimen were in a liquid-helium bath, and the upper critical field of niobium was easily achieved with this solenoid. Temperatures were determined from the vapor pressure of the bath. In this apparatus measurements could be made between 1.3 and 4.2°K.

B. Specimens

The Nb and Nb-Ta alloy specimens used in these experiments came from several different sources. They all were zone refined and outgassed in an ultrahigh vacuum. The In+1.9 at.% Bi sample was cast by putting the appropriate weight of bismuth and indium of 99.999% purity in a carbon mold. The specimen was annealed at 100°C for 3 weeks. The physical data for the specimens are given in Table I.

The residual resistivity ratio is proportional to the mean free path of the electrons at low temperatures. Ratios for Nb-2 and Nb-4 were measured using a four-lead potentiometric method, since the specimen cross sections were small. The Nb-3 and 50% Nb+50% Ta specimens were measured using an eddy-current method.[23] At 4.2°K, a magnetic field of about 5000 Oe was applied to the specimens to quench the superconductivity. The resistance ratio for the In-Bi specimen was inferred from the measured T_c and K and the

[21] J. R. Clement and E. H. Quinnell, Phys. Rev. 79, 1028 (1950).
[22] R. I. Gayley, E. A. Lynton, and B. Serin, Phys. Rev. 126, 43 (1962).

[23] C. P. Bean, R. W. DeBlois, and L. B. Nesbitt, J. Appl. Phys. 30, 1976 (1959).

data of Kinsel *et al.*[24] The results of these measurements are summarized in Table I.

C. Results

(i) C_p of Nb in the Normal and Superconducting Phases

Although all the specimens were measured in both the superconducting and normal phases, the most complete data were obtained for Nb-3 because of its large mass. A plot of C/VT versus T^2 for this specimen is shown in Fig. 2. The curves are very similar to those of Leupold and Boorse.[25] The superconducting curve does not go to zero because the heat capacity of the addenda has not been subtracted from the data. A rough estimate of the addenda heat capacity was obtained from measuring two Nb specimens of different mass. When the heat capacity of the addenda was subtracted, the resulting curve did go through zero at $0°K$. Moreover, the data in the interval $2°K < T < 4°K$ agree with those of Leupold and Boorse.

The jump in the specific heat at T_c is $(\Delta C/VT)_{T_c}$ $= 1.52$ mJ/cc($°K$)^2. Using the Rutgers formula, $(dH_c/dT)T_c = 438$ Oe/$°K$. Assuming the parabolic dependence of $H_c(T)$, the resulting H_0 for Nb-3 is $H_0 = 2040$ Oe. The extrapolation of the normal specific-heat line to $T = 0°K$ gives $\gamma = 0.80$ mJ/cc($°K$)^2, when corrected for the heat capacity of the addenda.

The data in Fig. 3 were numerically integrated to find $H_c(T)$, since $C_s - C_n = VT/4\pi[d/dT(H_c dH_c/dT)]$, where C_s and C_n are, respectively, the specific heats of the superconducting and normal phases.[16] For $T = 0°K$,

FIG. 3. Specific heats of Nb-4. All measurements were made in an applied magnetic field of 1030 Oe. However, in one case the specimen was cooled to the lowest temperature before the field was applied, whereas in the other the specimen was cooled in the field and then measured.

$H_0 = 2125$ Oe. The maximum deviation from the parabola determined by H_0 and T_c was 1.7% at $(T/T_c)^2 = 0.58$.

The γ determined in these measurements is 10% larger and H_0 is 6% larger than the same quantities determined by Leupold and Boorse. The maximum deviation of $H_c(T)$ from a parabola was 1.7% compared to their 1.2%. Since the determination of these data was not of primary importance in this work, and a precise determination of the heat capacity of the addenda was not made, the agreement noted appears satisfactory.

The values of $(\Delta C/VT)_{T_c}$ determined for all the specimens are listed in Table I. These were used to find $H_c(T)$ as described in Sec. II.

(ii) Specific-Heat Data at H_{c2}

The specific heats of Nb-4 measured in a field of 1030 Oe are shown in Fig. 3. We discuss in this section the data in the neighborhood of the discontinuity which in this applied field occurs at $(T_H)^2 \simeq 53(°K)^2$. It is to be noted that the discontinuity is relatively abrupt, and the specific heat is reversible in this temperature region. That is to say, the same values were obtained independent of whether (a) the specimen was cooled
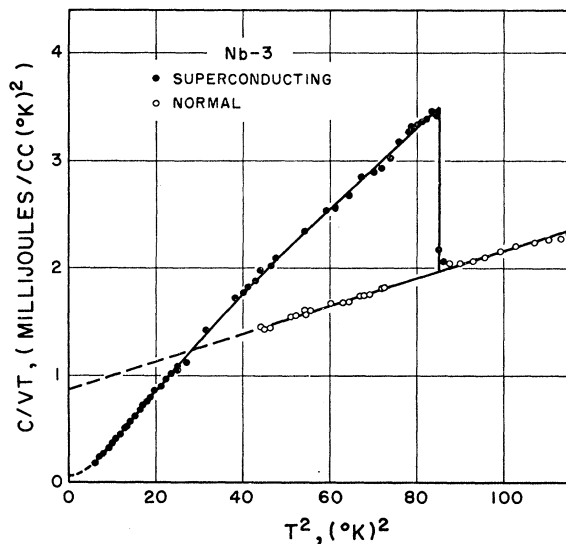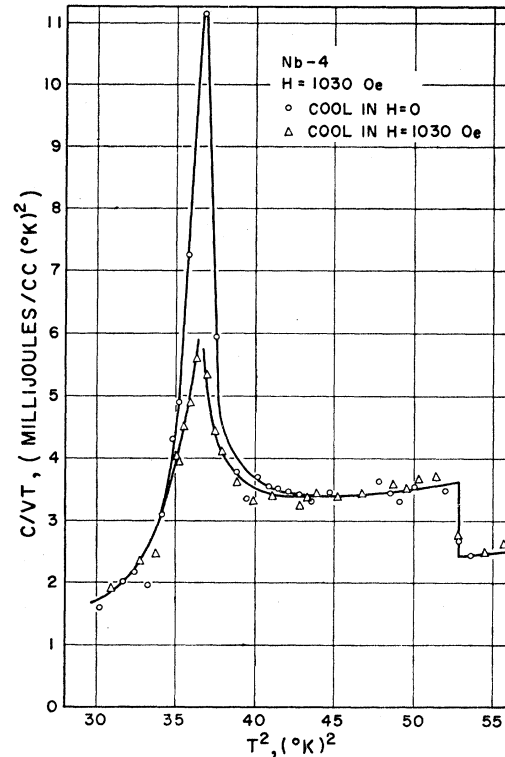

FIG. 2. Specific heats of niobium in the superconducting and normal phases.

[24] T. Kinsel, E. A. Lynton, and B. Serin, Rev. Mod. Phys. **36**, 105 (1964); T. Kinsel, thesis, Rutgers University, 1963 (unpublished).

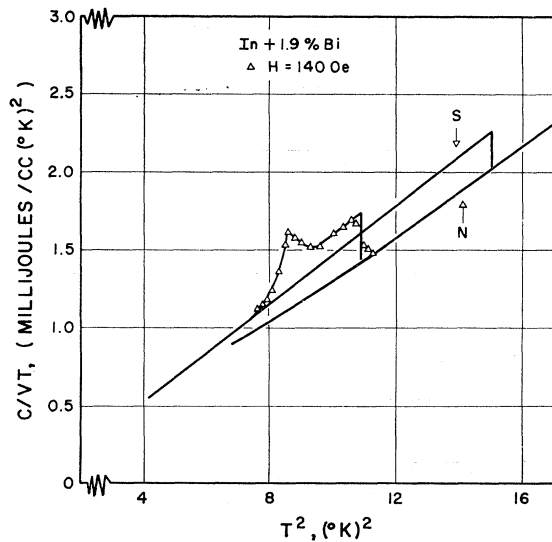[25] H. A. Leupold and H. A. Boorse, Phys. Rev. **134**, A1322 (1964).

Fig. 4. Specific heats of the In+1.9% Bi specimen in an applied magnetic field of 140 Oe. The specimen was cooled before the field was applied. Results for the normal (N) and superconducting (S) phases are shown. Data points were omitted to avoid confusion.

to the lowest temperature in zero field, the field applied, and measurements were made, or (b) the specimen was cooled in a field of 1030 Oe and then measured. All specimens, whether pure or alloy, were similarly reversible.

Figure 4 shows data for the In+1.9% Bi specimen in a field of 140 Oe. Also shown are the results of measurements in the superconducting and normal phases. Since the electronic specific heat of the In-Bi specimen is an order of magnitude smaller than that of Nb, the magnitude of the effects of the type-II behavior are correspondingly smaller. The data obtained were of sufficient accuracy to analyze the specific-heat jumps, but not to analyze meaningfully the normal state results.

From measurements such as these in various applied fields, values of $H_{c2}(T)$ and $(\Delta C/VT)_{T_H}$ were determined for all the specimens, and K_1 and K_2 calculated. The results are collected in Table II.

It should be noted that the In-Bi alloy was chosen to have nearly the same value K as the Nb specimens. There is, however, a difference of a factor of about 200 between the resistivity ratios for Nb-3 or Nb-4 and the ratio for the In-Bi alloy.

(iii) Magnetization Data for Nb-4

We show in Fig. 5 a magnetization curve at 4.21°K for one wire of Nb-4. Also shown on an expanded scale are the data near H_{c2}. The area under the curve in Fig. 5(a) should equal $H_c^2/8\pi$. From a numerical integration we obtain $H_c = 1608$ Oe. Using the value $H_0 = 2040$ Oe, obtained from the specific-heat jump, and the parabolic approximation for $H_c(T)$, we find that at 4.21°K $H_c = 1609$ Oe, in good agreement with the

value obtained from the magnetization curve. This agreement gives us added confidence that assuming a parabolic critical field curve does not seriously affect our conclusions.

Data of the type shown in Fig. 5(b) were obtained at several temperatures, enabling $H_{c2}(T)$ and $(dM/dH)_{H_{c2}}$ to be determined, and K_1 and K_2 to be calculated. The values obtained are listed in Table III.

The data for $H_{c2}(T)$ obtained from both the specific-heat and magnetization measurements are plotted in Fig. 6. It is to be noted that the values from the two types of measurements fit together reasonably well, and that H_{c2} is linear in $(T_c - T)$ within experimental error to quite low temperatures. We estimate $H_{c2}(0) = 3800 \pm 50$ Oe. Also, as can be seen from Figs. 6 and 7 and Table II, the data for Nb-3 and Nb-4 are indistinguishable to within the scatter, and we will treat them together.

(iv) Specific-Heat Peak

The large specific-heat peak indicating the entrance of magnetic flux into the specimen is shown in Fig. 3. We have found that the temperature at which the peak occurs in a given applied field varies greatly among the niobium specimens, occurring at the lowest temperature in Nb-4 and at the highest in Nb-2. The most extreme

TABLE II. The temperatures T_H are listed at which the specific-heat discontinuity ΔC is observed in the applied field H_a. The parameters K_1 and K_2 are calculated from the data.

H_a (Oe)	T_H (°K)	$t = T_H/T_c$	K_1	$(\Delta C/VT)_{T_H}$ [mJ/cm^3(°K)^2]	K_2	K_2/K_1
Nb-4:						
672	7.95	0.862	0.912	1.51	1.07	1.17
800	7.67	0.831	0.927	1.38	1.09	1.18
1030	7.24	0.785	0.952	1.17	1.15	1.21
1183	7.00	0.758	0.968	1.05	1.19	1.23
1470	6.51	0.705	0.995	0.83	1.28	1.29
Nb-3:						
200	8.81	0.955	0.870	2.87	0.913	1.05
300	8.63	0.935	0.879	2.27	0.960	1.09
400	8.44	0.915	0.887	2.03	0.986	1.11
593	8.09	0.877	0.906	1.55	1.05	1.16
792	7.71	0.836	0.925	1.35	1.10	1.19
1028	7.31	0.792	0.948	1.15	1.15	1.21
1187	7.01	0.760	0.966	1.01	1.20	1.24
1470	6.53	0.708	0.995	0.81	1.30	1.31
Nb-2:						
800	7.82	0.852	1.04	1.94	1.06	1.02
1030	7.45	0.812	1.06	1.61	1.12	1.06
1200	7.15	0.779	1.085	1.46	1.16	1.07
50% Nb+50% Ta:						
1030	5.77	0.924	4.05	1.05	3.92	0.969
1192	5.70	0.913	4.07	1.03	3.96	0.973
1470	5.60	0.896	4.11	1.06	3.92	0.955
In+1.9% Bi:						
60	3.62	0.935	1.01	0.40	0.983	0.974
100	3.44	0.891	1.03	0.37	1.01	0.980
140	3.28	0.849	1.05	0.33	1.04	0.990
160	3.19	0.827	1.07	0.31	1.06	0.990
200	3.02	0.781	1.09	0.29	1.08	0.990

FIG. 5. (a) Magnetization of Nb-4 at 4.21°K. (b) The data in the neighborhood of the upper critical field are shown on an expanded scale.
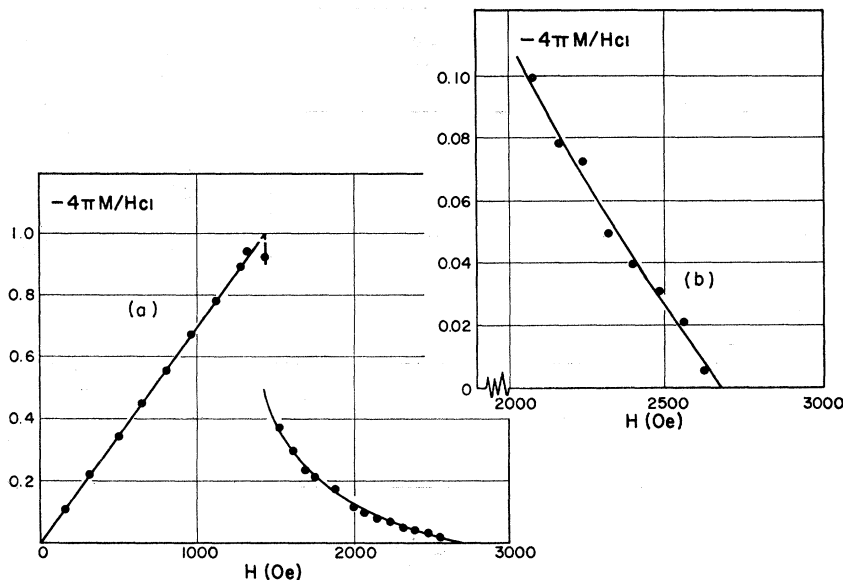
case occurred in the first specimen we measured,[10] Nb-1. In this specimen the peak and the discontinuous drop to the normal state occurred at the same temperature, and led us initially to incorrect conclusions concerning the properties of Nb. The temperature at which flux entry occurs has no clear relationship to the resistivity ratio of the specimens. Moreover, the specific heat in the neighborhood of the peak is generally irreversible. Only in the specimen Nb-4 was some peaking observed when the specimen was cooled in a magnetic field before it was measured. Delayed flux entry of the type described above has been shown to be very sensitive to the presence of structural defects in specimens.[26] It is possible that the position of the peak of Nb-4 represents the limit where the entry of flux is not delayed, but we cannot be sure that this is so. For this reason, we have not attempted to acquire detailed data on the dependence of the lower critical field on temperature for comparison with theory.

The data in Fig. 3 do indicate that in an ideal niobium specimen a very large reversible specific-heat peak would be present when flux entered the specimen. A complementary aspect of this behavior is the rapid

drop in magnetization over a small field interval near the lower critical field illustrated in Fig. 5. We have found that the entropy change associated with the area under the peak is consistent with the observed change in magnetization. These results raised the question as to whether the phase transition at H_{c1} is of the λ type or a broadened first-order transition with a latent heat. We were unable to decided this question by specific-heat measurements on the specimens available to us. However, one of us[27] recently made detailed magnetization

Table III. Data obtained from magnetization measurements on one wire of Nb-4. (H_{c2}=upper critical field, and $(dM/dH)_{H_{c2}}$= slope of magnetization curve at H_{c2}.)

T (°K)	$t=T/T_c$	H_{c2} (Oe)	$(dM/dH)_{H_{c2}}$	K_1	K_2	K_2/K_1
4.21	0.456	2680	0.0166	1.18	1.59	1.35
3.46	0.374	3015	0.0144	1.22	1.69	1.385
2.80	0.303	3300	0.0131	1.25	1.74	1.39
2.12	0.228	3540	0.0128	1.30	1.77	1.37
1.51	0.163	3625	0.0123	1.29	1.80	1.39

[26] J. Silcox and R. W. Rollins, Rev. Mod. Phys. 36, 52 (1964); J. D. Livingston, ibid. 36, 54 (1964).
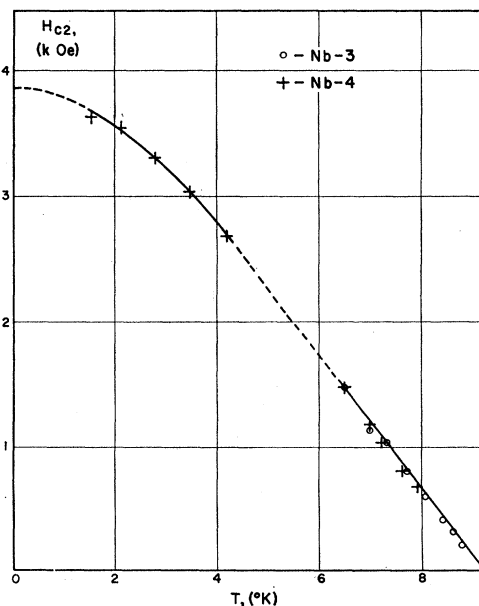

FIG. 6. Upper critical fields for the two purest niobium specimens. The high-temperature data were obtained calorimetrically, and the low-temperature data from magnetization curves.
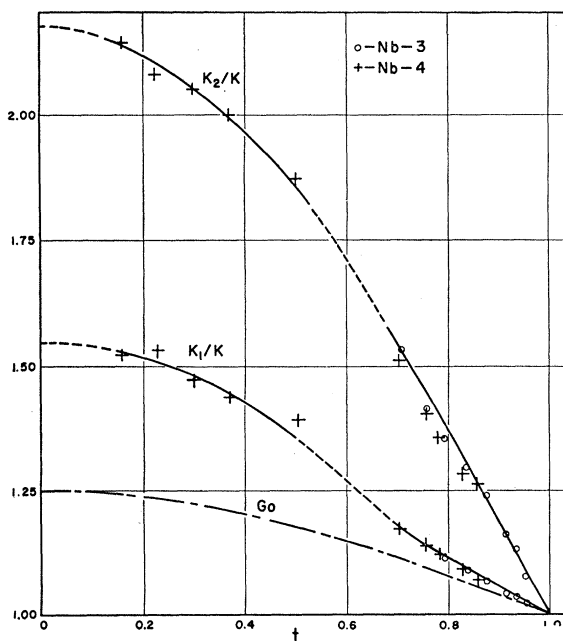
[27] B. Serin, Phys. Letters 16, 112 (1965).

FIG. 7. K_1 and K_2 are shown as a function of the reduced temperature. K is the Ginzburg-Landau parameter at the transition temperature. The high-temperature data were obtained calorimetrically, and the low-temperature data from magnetization curves. The curve marked Go is the theoretical expression for K_1/K due to Gor'kov (see Ref. 4).

measurements very close to H_{c1} on a wire of Nb-4. These measurements clearly indicated that the magnetization has a logarithmically infinite slope on the high field side of H_{c1}. This result implies that the specific heat indeed exhibits a λ point. We note that there is clear evidence for a peak in the In-Bi alloy specimen, so that it seems reasonable to infer that all type-II superconductors should ideally exhibit a λ point at the lower critical field.

IV. DISCUSSION

It is clear from Tables II and III that for Nb-3 and Nb-4, K_2 exceeds K_1 at all temperatures below T_c. For the alloy specimens, on the other hand, there is no clear indication of this behavior, and to within experimental scatter we conclude that $K_2 \sim K_1$. We note that K_2 also exceeds K_1 for the specimen Nb-2, but that at the same reduced temperature, K_2/K_1 is less for this specimen than for the other two niobium specimens. Recalling that the resistance ratios decrease monotonically in the order that the specimens are listed in Table II, we see that we have here evidence for a clear effect of electron mean free path on the magnetic properties of type-II superconductors.

Maki and Tsuzuki[15] have recently derived the result that K_2 should exceed K_1 in "intrinsic London superconductors." In order to compare theory and experiment, we show in Fig. 7 the experimental values of K_1/K and K_2/K plotted as a function of reduced temperature. K was obtained extrapolating the data for

K_1 and K_2 to a common value at $t=1$; the values obtained are listed in Table I. There is a hiatus in the data between 4.2 and 6.5°K, and we are not sure that the sigmoid character of the curve drawn for K_1 is real, but the general trend is clear. The temperature dependence of K_1 obtained by Maki and Tsuzuki is identical to that derived by Gor'kov[4] several years ago. Moreover, the same result for the intrinsic case has been obtained by Helfand and Werthamer,[28] and by Tewordt[29] for $T \sim T_c$. This agreement is not surprising, since all the authors started from the same basic assumptions. We show in Fig. 7 the theoretical curve. As can be seen, the data at all temperatures fall higher than predicted by the theory. In particular $K_1(0) \simeq 1.5$ whereas the prediction is 1.25. It is our opinion that the discrepancy between theory and experiment reflects the neglect of some fundamental aspect of the problem in the theoretical treatment, probably the failure to treat adequately nonlocal electrodynamic effects. In an independent investigation Chang[30] has obtained data on type-I superconductors which again clearly show that the temperature dependence of K_1 in pure specimens is more rapid than predicted by this theory. As for the temperature dependence of K_2/K, Maki and Tsuzuki[15] predict that the slope near $t=1$ should be -2.36, whereas near $t=0$, K_2 should vary as $[\ln(1/t)]^{1/2}$, in an ideal specimen. In any real specimen, it is expected that scattering of the electrons by defects will make the logarithmic singularity unobservable and result in a finite value of K_2 at low temperatures. Experimentally, the slope of the curve in Fig. 7 is -3.5 at $t=1$, appreciably larger than the theoretical slope. As expected K_2/K approaches a finite value (of about 2.2) at $t=0$. We note that both K_1 and K_2 are larger than K at all temperatures below T_c.

Maki[14] has predicted that type-II superconductors of very short electron mean free path should behave quite differently from the intrinsic variety. In particular, he obtains $K_2 < K < K_1$ at all temperatures below T_c. As already stated, the data in Table II for the alloy specimens indicate $K_2 \sim K_1$. It is clear that for the In-Bi specimen both these parameters increase as the temperature is lowered, so that K_2 exceeds K below T_c. Since the data in this investigation do not extend to very low temperatures, we have carefully examined the magnetization data of Kinsel[24] for indium bismuth alloys which were measured down to $t \sim 0.3$. These also indicate $K_2 \sim K_1$ at all temperatures. We note that we have found that the transitions near H_{c2} tend to be reversible, so that values of K_2 obtained from the slopes of magnetization curves near the upper critical field are probably reliable. Moreover, the calculation of K_2 from the slope does not require a knowledge of $H_c(T)$. All of

[28] E. Helfand and N. R. Werthamer, Phys. Rev. Letters 13, 686 (1964).
[29] L. Tewordt, Z. Physik 184, 319 (1965).
[30] G. K. Chang, thesis, Rutgers University 1964 (unpublished); G. K. Chang and B. Serin, Bull. Am. Phys. Soc. 10, 44 (1965).

Kinsel's data show an increase of K_2 of at least 12% between $t=1$ and $t\sim0.3$. On the basis of these results, we conclude that the weight of experimental evidence contradicts the theoretical inequality, $K_2<K$, for alloy type-II superconductors.

Superconducting Technetium-Tungsten Alloys*

S. H. AUTLER AND J. K. HULM

Westinghouse Research Laboratories, Pittsburgh, Pennsylvania

AND

R. S. KEMPER

Pacific Northwest Laboratories, Richland, Washington

(Received 23 June 1965)

The transition temperatures, critical fields, electrical resistivities, and crystalline structures of a series of technetium-tungsten alloys containing up to 60 at.% technetium are reported. T_c increases monotonically to 7.9°K and H_{c2} (at 4.2°K) to 43.5 kG for 60 at.% technetium. The samples are single-phase solid solutions up to 40 at.% Tc, but a sigma phase is present at higher concentrations. The measured values of H_{c2} are in good agreement with calculated values based on the BCS and Ginsberg-Landau-Abrikosov-Gor'kov theories and with our resistivity measurements.

INTRODUCTION

VIEWED as a superconductor, the element technetium is fascinating. It has the highest transition temperature for a hexagonal metal and the second-highest transition temperature (circa 8°K) for any element, being exceeded only by niobium (9.25°K). In view of the extensive formation of useful type-II compounds and alloys by niobium, it would be surprising if technetium could not be used as a base for interesting type-II superconductors. However, this possibility has only been examined to a limited extent, and, although the transition temperatures have been determined for a few technetium alloys,[1] no critical-field data exist in the published literature.

With a view to remedying this deficiency we have recently begun to explore the superconducting properties of various technetium alloy systems in more detail. The present paper describes some measurements on the tungsten-technetium system. The data presented include transition temperature, upper critical field and electrical resistivity at room temperature.

EXPERIMENTAL DETAILS

The initial starting materials[2] were in powder form with typical impurity contents shown in Table I. Suitable mixtures of these powders were loaded into a rubber compacting die and pressed at about 70 000 psi. Initially the pressed compacts were melted in a water-cooled copper-hearth arc furnace with a tungsten electrode and an argon atmosphere. This procedure was unsatisfactory due to poor conductivity in the compact and extensive oxide evolution. Therefore the later compacts were presintered in hydrogen at 1000°C for about one h, which greatly lowered the oxygen content and made arc melting much easier. The resulting buttons

TABLE I. Purity of starting materials (parts per million, typical values).

Material\Impurity	O	N	H	Major metals
Technetium	1260	20	39	Fe 50, Al 50, Si 20, Na 20, Ca 5
Tungsten	2411	106	⋯	Ni 30, Mo 21, Ca 11, Na 11, Fe 5

---

[1] V. B. Compton, E. Corenzwit, J. P. Maita, B. T. Matthias, and F. J. Morin, Phys. Rev. **123**, 1567 (1961).

[2] A more detailed account of the specimen preparation is given in Atomic Energy Commission Research Report No. HW-84550, 1965.